Feasibility Analysis of Replacing Overhead Transmission Lines with DC Underground Cable to Enhance Microgrid Resiliency

Senior Design Project: EE 461 in Fall 2020 and EE 462 in Winter 2021

Students: Amy La, Gerardo Parra, Matthew Suen, and Lucas Rasmussen

Advisor: Dr. Majid Poshtan

Sponsors: EPRI GridEd and CYME

Electrical Engineering Department
California Polytechnic State University in San Luis Obispo

ACKNOWLEDGMENT

The senior design student team and the project advisor, Professor Majid Poshtan, would like to thank the Center for Grid Engineering Education of Electric Power Research Institute (EPRI-GridEd), CYME, Cal Poly Sponsored Programs, and the EE Department for their support of this project. The team completed the project using CYMCAP, ETAP and LVSIM software simulators.

1. INTRODUCTION AND ABSTRACT

Underground lines have numerous benefits that are more prevalent in situations usually dominated by overhead lines. Specifically, they promote grid resiliency in wildfire mitigation and other kinds of hazards. They are other microgrid network structures that establish manageable power delivery and encourage renewable sources. Underground cables create a better living environment concerning environmentally friendly power and aboveground infrastructure. In California, a rising danger is wildfires caused by overhead power lines. By relocating and installing new electrical networks underground, risks caused by potential faults and arcs can be removed entirely. The design of an underground transmission route between a future Gold Tree Solar Farm and Cal Poly's EE microgrid is the first phase of our network design. In this phase, we use CYMCAP to study and choose the best underground cable. Our goal is install such cables that their installation and location would be beneficial to the loads at the microgrid. The second phase of the project is to design a wind farm for power generators to increase the active and reactive power of the microgrid. In the second phase, we use LVSIM software to study the performance of wind power generators as the second source of the power beside the Gold Tree Solar Farm.

2. CABLE MODELING

The control cable is a copper 69 kV underground power cable selected from Southwire Cable's selection of HV underground products. We have expected that the line voltage would be best at a lower transmission voltage because of the small length of the transmission route. This cable design, completed in CYMCAP with a compacted stranded conductor, conductor shield, XLPE insulation (with insulation shield), corrugated copper sheath, and a polyethylene jacket. Southwire provided the specs of the cables including the conductor diameter, insulation thickness/diameter, and overall jacket diameter. The smallest given conductor size of 500 kcmil was used for this model. At 69 kV, we have determined that this size was adequate. We modified the selected cable to 1000 kcmil and then switched the conductor to aluminum. We also studied a 12 kV transmission line so that there is no step down necessary to distribute power throughout EE Microgrid. Another cable, this time from Keystone, was selected. The components of this cable are primarily the same— compacted copper with conductor shield and XLPE insulation, but it is three core instead. A supposed advantage of using a 12 kV line would be that single cable transmission would be possible if the cable can handle the current. This cable also contained a copper tape screen, steel tape armor, and a PVC sheath [2]. Besides conductor, insulation, and armor sizes, assumptions were made to model the rest of the component sizes. The mid-sized 13 mm conductor version was used. Each CYMCAP study typically followed the build process: In this project we used a 0.75 load factor (based on Southwire's ampacity measurements), 20 ° C ambient temperature, and a 90 ° C operating temperature. Duct bank materials were defaulted at concrete fill and with PVC ducts. Thermal resistivity of surroundings were defaulted to one mili-C/W, as figures for thermal resistivity of relevant soils and materials were not yet found. The duct bank and cable models were then selected. The following figure shows the results of the ampacity and temperatures for each phase. In the figure the magnetic field showing the center peak of its strength and the cancellation of the magnetic field. More detailed information, including steady state, electrical, and short circuit data, was obtained in CYMCAP's auto-generated reports.

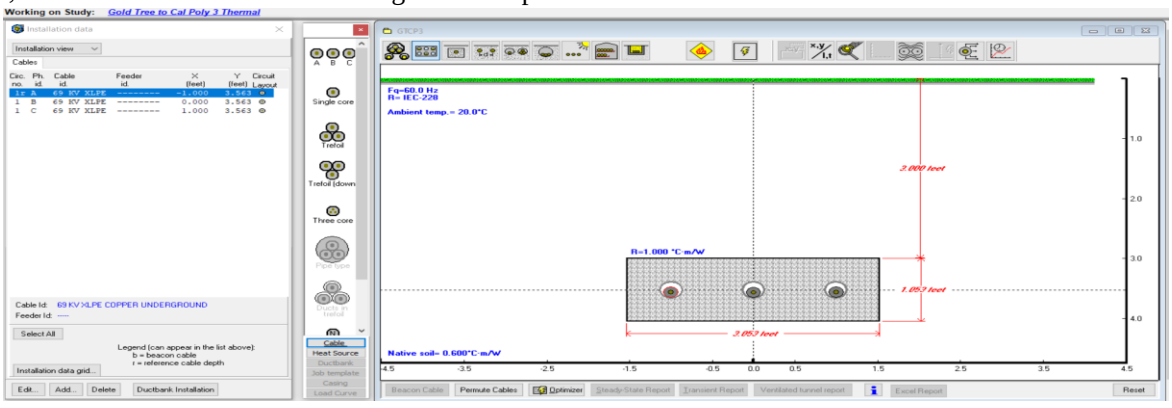

Figure 1. Standard Cable Study Screen in CYMCAP

Because the reports are extensive, data from the control, study specifically will describe the main measurements that were analyzed. Table 1 shows the how each change from the control study affected specific parameters.

Table **1:** Qualitative Comparisons of Studies

Study	Normal	Wider Ductbank	Shorter Ductbank	Direct Burial	Larger Conductor	Aluminum Conductor	12 kV Conductor	Lower Thermal Resistivity	Transposed
Ampacity	Base	Higher	Lower	Higher	Higher	Lower	Lower	Higher	Lower
Temperature	Base	Higher	Lower	Lower	Lower	Base	Higher	Lower	Base
Reactance		Higher	Lower	Base	Lower	Base	Lower	Base	Base
Magnetic Field	Base	Higher	Lower	Base	Higher	Lower	N/A	Higher	N/A
Capacitance	Base	Base	Base	Base	Higher	Base	Higher	Base	Base
Inductance	Base	Higher	Lower	Base	Lower	Base	Lower	Base	Base
Voltage Drop	Base	Higher	Lower	Lower	Lower	Higher	Higher	Lower	Base
Power Loss	Base	Higher	Lower	Higher	Higher	Base	Higher	Higher	Lower
SC Values	Base	Base	Base	Higher	Higher	Lower	Lower	Base	Base

The steady-state ampacity of a high voltage underground cable system is directly related to its ability to dissipate heat into its surroundings. This includes certain factors involving both the cable and installation design. Heat is generated in the metallic components of the cable and its insulative components. In terms of power, this heat is described in different ways mathematically.

Conductive: $W = R_{AC}(f,T) * I^2$

Insulative: $W = G(f,T) * V^2 = wCV^2 tan(\delta)$

In these equations, resistance and conductance are functions of frequency and temperature [3].

Our goal is to achieve max operation losses of no more than 10% of transmitted voltage and 5% of transmitted power. Because these losses were calculated with ampacity measurements in mind, these represent the max potential losses at operating currents. Voltage drop and power loss were given in the report in units of [V/A/mile] and W/ft, respectively, as line, resistance and current are the two primary factors influencing these losses. Specifically, $P = RI^2$ is the equation that best represents the primary behavior for these losses. As the ampacity increases, potential power loss usually increases too. In some scenarios, the resistance of the cable may change more than the current so that the voltage drop can decrease instead. For the standard study, these losses were valued at 0.57312 V/A/mile and 11.998 W/ft. considering an approximately 5-mile total route from the Gold Tree Solar Farm to EE Microgrid at an operating ampacity of about 630 A, these losses become a 1805 V / 316,737 W loss per phase. These losses are 4.53% and 5.9%, respectively, about the approximately 16 MVA, 69 kV line. However, these losses will decrease with normal operating currents expected to be around 133-Amp. Besides the cable's impedance, these losses can also be partly due to capacitive and inductive losses. The equation represents the capacitance of each cable

$$C = 2\pi\varepsilon_o\varepsilon_r * l/ln(b/a)$$

Capacitance increases when the distance between cables, b, decreases and the cable's size increases. This effect is not seen when the duct bank width is changed because the sheath blocks the electric field of the cables. The inductance of each cable follows a similar but opposite trend. The representative equation is

$$L = (\mu_o\mu_r/2\pi) * l * ln(b/a)$$

Inductance increases as b, the distance from the cable increases, or a, the cable width decreases. The magnetic field, which can interfere with surrounding equipment, correlates to the inductive effect of the cables. Although the field peaks in the center of the cable bundle and decreases quickly as it ventures farther out, the magnetic field cancellation of the bundles worsen the further apart they are. The triple core cable does not have a magnetic field due to only experiencing self-induction. From these effects, capacitive current discharge was calculated at 5.45209 A/mile, and induced sheath voltage at 199.52 V/mile. At ampacity, these losses are 27.26 A and 997.6 V total for an assumed 5 mile transmission route. The short circuit current capacity of a cable depends on the heat dissipation of the cable itself, meaning entirely based upon the conducting material's properties. Short circuits are calculated when the cables are operating at a max fault temperature of 250° C. If the cable is larger, has better sheath material, or is in cooler surroundings, heat capacity increases with the short circuit current. If the cable is smaller or is of a weaker conductor or sheath, heat capacity decreases with the short circuit current.

3. Cable Installation Design

Two methods of installation, Duct Banks and Direct Burial, were studied. We began our study with a "standard" duct bank with 12" of spacing between each cable. To analyze the effects of cable spacing, we also implemented studies of duct banks with spacing of 6" and 24". When decreasing the spacing between cables the ampacity decreased. However, we did also see a decrease in temperature, magnetic field, inductance, voltage drop, and power losses. When increasing the spacing of the cables it had a complete opposite effect since the ampacity, temperature, magnetic field, inductance, voltage drop, and power losses all increased. Reference Table 1 below for a qualitative comparison of the different duct banks. All of these qualitative measurements are taken

into consideration when deciding on the most appropriate cable installation. For example, although direct burial provides a higher ampacity and lower temperature, voltage drop, and power losses, it provides little to no protection for the underground cable. It introduces the risk of contact or damage during other underground work in the same area. Also, the cost of maintenance would be larger due to the necessity of recurring trench digging. In regards to duct bank cable spacing, the ampacity rating should not have to be as high if we have a 69kV operating voltage. Therefore, we could have a smaller duct bank to make it more compact and use less material. Assuming EE Microgrid's entire load is about 16MVA then we would have a current of approximately 133A flowing through our transmission lines at a 69kV operating voltage. This is not close to the ampacity ratings calculated in these cable installation studies so there is no expected risk of overloading the cable.

4. Cable Composition Design

Concerning the 69 kV cable, the cable size of 500 kcmil is already expected to be the optimal size for this route. The larger 1000 kcmil cable boosted the ampacity from approximately 630 A to 675 A. Despite the larger current carrying capacity, there is no present need for a larger cable. Smaller cables are not available and therefore not included in the study. In comparison, the study on an aluminum conductor proved to be more useful. The aluminum cable expectedly has an approximately 100 A decrease in ampacity at the same operating temperature but with either no change or improvements in nearly every performance category. In addition, aluminum is cheaper, weighs less, and is more resistant to mechanical stresses. These qualities make aluminum a good material for this transmission route that does not require copper's marginally better thermal and conductive properties. The 12 kV, three-core cable had the largest decrease in ampacity — from above 600 A to about 280 A. At this level, the current of our system is expected to approach or even exceed the ampacity rating. Due to the smaller voltage rating and conductor sizes, power loss and most other cable parameters would worsen with the exception of reactance and inductance. However, the multi-core build has some advantage over the other single-phase lines. Due to the need of only needing one line, three-core cables are both more expensive and easier to lay. They can also be armored, making them more resilient to mechanical stresses and able to be buried directly in the ground. Due to our preferences towards using a duct bank and high voltage, these advantages are unnecessary.

5. Thermal Resistivity Analysis

The composition of the cable surroundings also have a substantial effect on its performance. When considering the effects of thermal resistivity, there are three areas that must be taken into consideration: native soil, concrete used for the duct bank and backfill material. Most studies use a soil thermal resistivity (rho) of 90 C-cm/W as standard practice when the native soil is also used as backfill [5]. Damp soils have a rho of less than 90 C-cm/W while moist sands have a rho of less than 50 C-cm/W, but may dry considerably when heated. Dry soils can exceed 150 C-cm/W and possibly reach levels of 300 C-cm/W. Soil surveys in the coastal region of California have shown that the native soil has a rho value of around 60 - 90 C-cm/W since this area is quite damp. Properly designed and installed soil backfill should have a dry thermal rho of less than 100 C-cm/W, potentially as low as 75 C-cm/W. Cable backfill materials should preferably maintain a low thermal resistivity of less than 50 C-cm/W that is lower than most native soil even while subjected to high temperatures for prolonged periods.

6. Transposition

When the spacing of three phase transmission lines are unequal, the admittance and capacitance of different phases are also different with each other The uneven distribution and unbalanced transmission line impedance would lead to an unbalanced system that could worsen as the distance of the line gets larger [7]. Transposition, a spatial rotation of transmission line, is the solution to this problem. Usually, the whole system would be divided into three segments and transposition would be done for three times. For instance, in a three-phase system, a-phase would be transposed to b-phase and then transposed to c-phase. The exchange of the position of the cable neutralizes the unbalanced inductance and capacitance so that the power system can achieve the same magnitude with 120 phase shifts [8]. In CYMCAP, a dedicated transposition selection option was not located. The best approach for virtually transposition is by using the trefoil formation, which will get the same result as the transposition in theory. CYMCAP assumes that the cables are transposed in trefoil formation. In the resulting study report, the voltage drop for the three-phase system for all the three cables is expectedly the same. It is noticeable that the capacitance, reactance, and the inductance of the conductors were the same no matter what differences in bonding or spacing were present. The parameter leading to the difference in voltage drop is the impedance of the three cables. The sheath binding type such as single point or cross bonding must be taken into consideration. In CYMCAP, the transposition of single conductor cables reduces the circulating currents in the sheaths when cables are bonded at both ends and they are arranged in flat formation (single conductor sheath bonded end, flat configuration). It is relevant only when the single-core cables are specified as being two point bonded. Single core cables in triangular formation are assumed transposed. For cross bonding, it is assumed only the sheaths were transposed and the cable not being transposed. The major difference for spacing evenly distributed and unevenly distributed is that the induced current on Metallic Screen of spacing unevenly is greater than that of spacing evenly. For transposed cable, in most of the cases, the value of cable 2 is higher than the value of cable 1 and 3 while the value of cable 1 and 3 are the same. It is not as expected.

7. NETWORK DESIGN

We use ETAP to create a complete design of our network and run network analysis that considers the differences and/or compatibility between AC and DC systems. System protection is performed for major types of protection. We explored functions in GIS that allowed us to map EE Microgrid's high voltage, gas and water networks. Since the CAD files do not provide 3-D information, we planned the pre-existing networks are placed underground to avoid interference. We exported the GIS information as CAD data and transfer that to ETAP.

8. PROTECTION

There are several protective devices, which are used in this network. They include protective relays, circuit breakers, current transformers, and voltage transformers. A protective relay is used to detect any fault or abnormal condition of the transmission line including short circuit or overloads. In most of the distribution system, current sensing devices such as overcurrent relay a re used as the major protective device. Using CYMCAP, we calculated their effects on the primary electrical properties of the line. Each change is analyzed using report data from CYMCAP.

9. CAL POLY EE MICROGRID

A microgrid is a local energy grid that could be disconnected from the larger grid and operate autonomously. This particular segment of the power industry is growing due to its reliability during times of emergency and crisis. Among these benefits are improved efficiency, lower operating cost, renewable generation sources, and improved resiliency of the regional electric grid. Communities are able to better prepare for unprecedented weather such as wildfires, hurricanes, and other natural disasters. Regions that produce renewable energy can export their surplus through high voltage transmission lines to balance power supply and demand needs. This Underground High-Voltage Transmission Network project aims to design a blueprint for an underground high voltage transmission network that will eventually connect Gold Tree Solar Farm to the Cal Poly EE microgrid via an underground network. The solar farm generates 25% of the microgrid's load, which makes it essential to everyday operations on the microgrid. The project develops methods to examine network resiliency and analyze load growth or demography trends. These methods include using GIS to properly locate any existing underground infrastructure and utilizing CYMCAP software to size cable. ETAP software are utilized to perform load flow analysis and device coordination simulation.

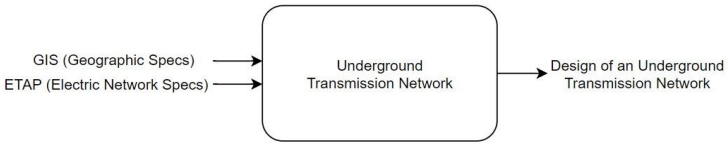

Figure 2. Level 0 Block Diagram.

The following table records and analyzes the inputs/outputs and describes the functionality of these components working together.

Table 2. Level 0 Functionality for the Network

Level 0 Module	Underground Transmission Network
Input	GIS (Geographic Information System) ETAP (Electrical Power System Analysis Software)
Output	Customer Power
Functionality	Using ETAP and GIS we are able to develop a feasible blueprint design that provides renewable energy, an underground transmission network, smart control, system protection and security.

Our Level_1 block diagram expands the scope of the network's functionality (Figure 2). Because GIS and ETAP are the system's inputs. We defined the software as tools for two microgrid design concepts— line placement and network design. Concerning using GIS for line placement, geographical obstacles must be determined before completing cable design. We used ETAP for power flow in the underground transmission line network.

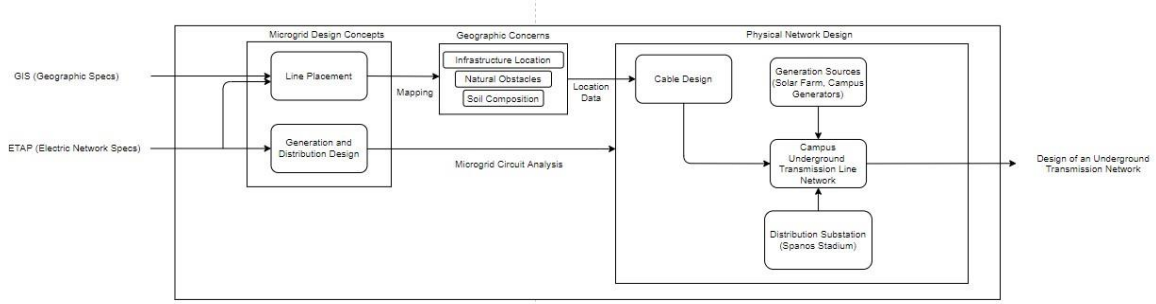

Figure 3. Level 1 Block Diagram